

Innovation

Precise Platform Positioning with a Single GPS Receiver

Sunil B. Bisnath, Tomas Beran, and Richard B. Langley University of New Brunswick

With the removal of Selective Availability about two years ago, the twice-distance root-mean-square horizontal accuracy of single-receiver, single-epoch GPS point positioning afforded by the Standard Positioning Service has improved to better than 10 meters in many situations. Differential positioning techniques and the use of carrier-phase data can provide higher accuracies, even to sub-centimeter levels. However, these techniques require raw data or corrections from another receiver. The subject of this month's column is the design of a GPS data processing technique capable of producing positions with accuracies at the few-decimeter level using data from a single receiver, regardless of platform dynamics. This feat is accomplished by combining two processing philosophies: point positioning – making use of precise GPS constellation ephemeris and clock offset information to estimate a single receiver's state; and carrier-phase-filtered, pseudorange processing – supplementing pseudorange-based positioning with carrier-based position-change information.

To discuss the technique and its applications, I am joined by two of my graduate students, Sunil Bisnath and Tomas Beran. Sunil Bisnath received an Honours B.Sc. in 1993 and an M.Sc. in 1995 in Surveying Science from the University of Toronto. For the past six years he has been a Ph.D. candidate in the Department of Geodesy and Geomatics Engineering at the University of New Brunswick. During this time he has worked on a variety of GPS-related research and development projects at the Department's Geodetic Research Laboratory, the majority of which have focused on the use of GPS for space applications. Tomas Beran is also a Ph.D. student in the same department where he has been working on his degree since 1999. He received his Master's degree from the Czech Technical University in Prague. His main research area is low-cost spaceborne single-receiver GPS positioning.

A primary application of GPS is the precise positioning of a myriad of differing user platforms over a broad spectrum of environments, on and above the Earth's surface. Current processing techniques rely on relative positioning between receivers, carrier-phase ambiguity resolution, differential receiver corrections, or spatial interpolation of receiver network information, implemented in dynamics-tuned filtering schemes to greatly improve position accuracy over that provided by the Standard Positioning Service.

The potential of point positioning is that it can remove these cumbersome aspects of GPS positioning for many applications. We have devised a novel approach which obviates the need for these techniques by using data from only the user receiver and products of the International GPS Service (IGS).

This approach is not adversely affect-

ed by the decorrelation of biases in relative or differential positioning, unresolved phase ambiguities, spatial interpolation errors, or assumptions regarding platform dynamics, and only requires the tacit assumption of sufficient GPS signals for positioning.

In this article, we discuss first the concepts of point positioning and pseudorange and carrier-phase processing. Then we describe our single-receiver, platform-independent processing strategy; discuss several tests with terrestrial, airborne, and spaceborne data; give conclusions, and specify plans for future research.

Point Positioning

The original intent for GPS usage was single-receiver, real-time, pseudorange-based positioning. As is well known, this original design has been altered and enhanced by the use of the carrier-phase

observables, relative positioning, and differential positioning on local and wide-area scales. In recent years some researchers have turned their focus to point positioning again. With the proliferation of regional and global networks of geodetic-grade GPS receivers, such as the IGS network, precise GPS satellite orbits and in some cases precise satellite clock offset estimates derived from such networks have been used to produce precise positioning results with a single receiver. Mathematically, the GPS satellite ephemeris and clock parameter errors can be removed from the positioning functional model.

Work in this area first centered on pseudorange-based positioning, and then more recently on pseudorange and carrier-phase processing. The carrier-phase strategies have involved the estimation of the receiver state, undifferenced phase ambiguities, and other parameters.

In our approach we have avoided the ambiguity estimation process by utilizing adjacent-in-time-differenced phase measurements. This represents a form of phase-smoothed pseudorange positioning. The rationale for such a formulation, as will be seen, is to eliminate the necessity for dynamic modeling of the platform.

Pseudorange Processing

A number of researchers have proposed and/or developed carrier-phase-filtered, pseudorange processing techniques. Their basic form can be attributed to the seminal work of Ron Hach back in the early 1980s. The crux of carrier and pseudorange combination is the use of averaged noisy code-phase range measurements to estimate the ambiguity term in the precise carrier-phase range measurements. The longer the pseudorange averaging, the better the carrier-phase ambiguity estimate. By performing the filtering in the positioning domain, rather than in the measurement domain, changes to the tracked satellite constellation have little effect as long as a continuous filtered solution is possible. In essence, the pseudoranges provide coarse position estimates and the relative carrier phase measurements provide precise position change estimates. The position change estimates are used to map all of the position estimates to one epoch for averaging.

Several authors have developed similar processing filters with a relative positioning formulation for terrestrial applications utilizing the double-differenced

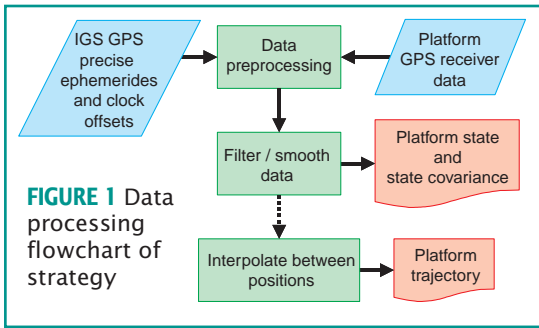


FIGURE 1 Data processing flowchart of strategy

ter of the GPS satellite antenna and the satellite center of mass; GPS satellite phase wind-up due to the relative rotation of the satellites with respect to the receiver; sub-diurnal variations in Earth rotation; solid Earth tides; ocean loading; and consistency between the models used in the generation of the pre-

cise GPS orbits and clocks, and those used in the point positioning processing.

Filter Models and Solution

The linearized filter observation model in matrix form is given by

$$\begin{bmatrix} \mathbf{P}_t - \mathbf{P}_t^0 \\ \delta\Phi_t - \delta\Phi_t^0 \end{bmatrix} = \begin{bmatrix} 0 & \mathbf{A}_t \\ -\mathbf{A}_{t-1} & \mathbf{A}_t \end{bmatrix} \begin{bmatrix} \delta\mathbf{x}_{t-1} \\ \delta\mathbf{x}_t \end{bmatrix} + \begin{bmatrix} \mathbf{e}_t \\ \boldsymbol{\varepsilon}_{t-1,t} \end{bmatrix};$$

$$\mathbf{C}_{P_t}, \mathbf{C}_{\delta\Phi_t}, \quad (1)$$

pseudorange and carrier-phase observables and the GPS broadcast ephemeris in a sequential, least-squares processor. Researchers at the Jet Propulsion Laboratory (JPL) and the European Space Agency proposed this type of filter in the mid- to late 1980s for determining GPS-based low Earth orbiter (LEO) trajectories. However, this strategy was abandoned for others, since at the time a global array of terrestrial GPS reference stations did not yet exist to provide sufficiently precise GPS ephemerides and clock estimates.

Filter Design

We have re-proposed this form of dynamics-free processing for single-receiver processing, utilizing only readily-available IGS data products and the mobile receiver measurements. This approach provides for very efficient, straightforward processing and takes full advantage of the precise, three-dimensional and continuous nature of GPS measurements, as well as the existing GPS data infrastructure.

Figure 1 shows the strategy's processing flow. The input pseudorange and carrier-phase data are pre-processed to detect outliers, cycle slips, and other problems in the data and then used to form the processing observables. The position of the mobile receiver is then estimated with the filter described in the following section. If necessary, an accurate interpolation procedure can be applied to provide the mobile receiver state estimates at non-GPS-measurement epochs.

The observables fed to the filter are the ionosphere-free, undifferenced pseudorange and the ionosphere-free, time-differenced carrier-phase. For point positioning, a number of additional modeling considerations must be taken into account above and beyond those required for relative positioning. These include the relativistic GPS satellite clock correction due to the eccentricity in the satellite orbits; the offset between the phase cen-

Innovation

where \mathbf{P}_t and \mathbf{P}_t^0 are the pseudorange measurement and predicted value; $\delta\Phi_t$ and $\delta\Phi_t^0$ are the time-differenced carrier phase measurement and predicted value; $\delta\mathbf{x}_{t-1}$ and $\delta\mathbf{x}_t$ are the estimated corrections to the receiver position and clock at epoch $t-1$ and t ; \mathbf{A}_{t-1} and \mathbf{A}_t are the measurement partial derivatives with respect to the receiver position and clock estimates for epochs $t-1$ and t ; \mathbf{e}_t and \mathbf{e}_{t-1} are the measurement errors associated with \mathbf{P}_t and $\delta\Phi_t$; and $\mathbf{C}_{\mathbf{P}_t}$ and $\mathbf{C}_{\delta\Phi_t}$ are the covariance matrices for \mathbf{P}_t and $\delta\Phi_t$. Note that at present, we assume the pseudorange and carrier-phase measurements to be uncorrelated between observables and between observations.

Since the troposphere is a significant contributor to the GPS error budget for

platforms within the troposphere, the UNB3 tropospheric prediction model is optionally used. The omission of residual zenith delay estimation causes biases in the position estimates which are, on average, approximately a few centimeters. A small improvement in positioning results can be obtained with such estimation.

Another error source not explicitly accounted for in our model is the pseudorange multipath. To mitigate the effect of this phenomenon, a variant of the pseudorange-minus-carrier-phase linear combination is used to estimate the pseudorange multipath plus noise variance. We use these variances to construct more realistic pseudorange stochastic models.

The best solution for Equation (1), in a least-squares sense, is

$$\begin{bmatrix} \hat{\mathbf{x}}_{t-1} \\ \hat{\mathbf{x}}_t \end{bmatrix} = \begin{bmatrix} \mathbf{x}_{t-1}^0 \\ \mathbf{x}_t^0 \end{bmatrix} - \begin{bmatrix} \mathbf{A}_{t-1}^T \mathbf{C}_{\delta\Phi_t}^{-1} \mathbf{A}_{t-1} + \mathbf{C}_{x_{t-1}}^{-1} & -\mathbf{A}_{t-1}^T \mathbf{C}_{\delta\Phi_t}^{-1} \mathbf{A}_t \\ -\mathbf{A}_t^T \mathbf{C}_{\delta\Phi_t}^{-1} \mathbf{A}_{t-1} & \mathbf{A}_t^T (\mathbf{C}_{\mathbf{P}_t}^{-1} + \mathbf{C}_{\delta\Phi_t}^{-1}) \mathbf{A}_t \end{bmatrix}^{-1} \times \begin{bmatrix} -\mathbf{A}_{t-1}^T \mathbf{C}_{\delta\Phi_t}^{-1} \mathbf{w}_{\delta\Phi} \\ \mathbf{A}_t^T \mathbf{C}_{\mathbf{P}_t}^{-1} \mathbf{w}_p + \mathbf{A}_t^T \mathbf{C}_{\delta\Phi_t}^{-1} \mathbf{w}_{\delta\Phi} \end{bmatrix} \quad (2)$$

where $\hat{\mathbf{x}} = \mathbf{x}^0 + \delta\mathbf{x}$ (the estimate is equal to the approximate initially assumed value plus the estimated correction); \mathbf{w}_p and $\mathbf{w}_{\delta\Phi}$ are the misclosure vectors for the pseudoranges and time-differenced carrier phases; and $\mathbf{C}_{x_{t-1}}$ is the receiver position and clock covariance based on the last epoch's observations.

The position estimate at the previous epoch, $t-1$, is used to estimate the position at epoch t and so on for the moving

platform. Equation (2) represents a kinematic, sequential least-squares filter. This filter is a special case of the Kalman filter. Simply put, from Equation (1) the pseudorange measurement contribution

$$\mathbf{P}_t - \mathbf{P}_t^0 = \mathbf{A}_t \delta\mathbf{x}_t + \mathbf{e}_t; \quad (3)$$

$\mathbf{C}_{\mathbf{P}_t}$ can be extracted along with the carrier-phase measurement contribution

$$\delta\Phi_t - \delta\Phi_t^0 = -\mathbf{A}_{t-1} \delta\mathbf{x}_{t-1} + \mathbf{A}_t \delta\mathbf{x}_t + \mathbf{e}_{t-1,t}; \quad (4)$$

$\mathbf{C}_{\delta\Phi_t}$

The terms in Equation (3) can be directly mapped to those of the Kalman filter measurement model, and with some rearrangement the terms in Equation (4) can be effectively related to those of the Kalman dynamic model. That is, the kinematic, sequential least-squares tracking filter behaves like a Kalman filter because the carrier phase measurements represent its dynamic model. Figure 2 illustrates the filter process.

Finally, if this tracking strategy is performed after-the-fact and not in real time, data smoothing can be performed. That is, the data arc can be processed in the forward and backward directions and the results can be optimally combined. The smoothed solution is

$$\hat{\mathbf{x}}_{s_t} = \mathbf{C}_f^{-1} \hat{\mathbf{x}}_{f_t} + \mathbf{C}_b^{-1} \hat{\mathbf{x}}_{b_t} \quad (5)$$

where $\hat{\mathbf{x}}_{s_t}$ is the smoothed parameter estimate, \mathbf{C}_f is the forward filter parameter covariance, $\hat{\mathbf{x}}_{f_t}$ is the forward filter parameter estimate, \mathbf{C}_b is the backward filter parameter covariance, $\hat{\mathbf{x}}_{b_t}$ is the backward filter parameter estimate. This is a fixed-interval smoother in which the trace of the smoothed parameter covari-

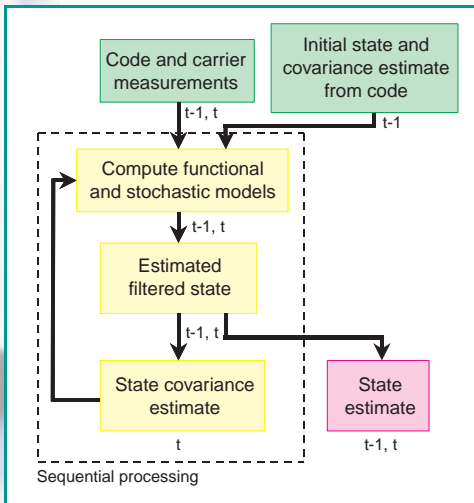


FIGURE 2 Combination of pseudo-range and carrier-phase observations in the kinematic, sequential least-squares filter

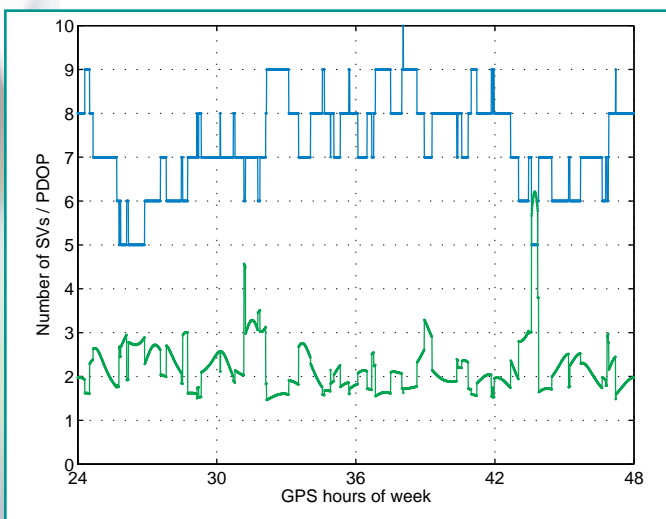


FIGURE 3 Number of space vehicles (SVs) and the position dilution of precision (PDOP) for static, terrestrial data set

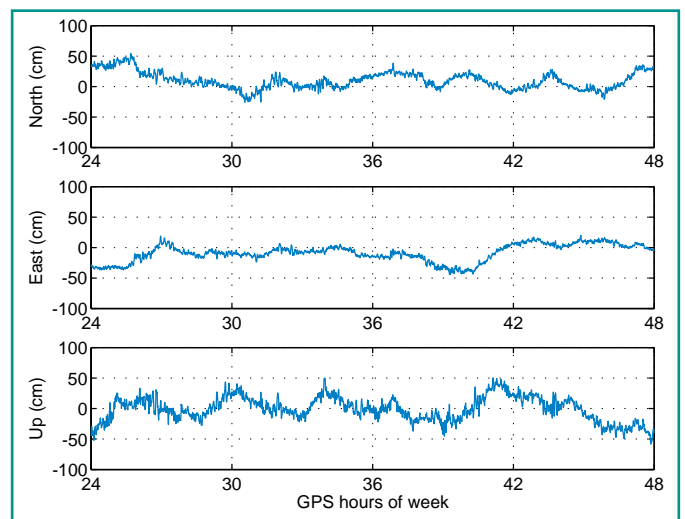


FIGURE 4 Component errors in smoothed position estimates for static, terrestrial data set

ance matrix is smaller than the trace of the covariance matrices of either filter.

Data Testing and Analysis

In order to validate the viability and performance of this strategy, we conducted a number of tests using the latest version of the processing software. This software, based on the University of New Brunswick's scientific GPS processing package DIPOP, consists of a compiled pre-processor and main processor. Even though the code was not designed to be optimal in terms of processing speed, all of the results presented were generated in minutes. Where applicable, we will mention additional processing or modeling that, with future development, should improve the accuracy of the results.

To illustrate the platform-independent nature of the technique, three widely varying types of data have been processed: terrestrial, airborne, and spaceborne. The only common (and required) characteristic of these data sets is that they were collected with geodetic-grade receivers – that is, the receivers were capable of measuring high-quality (low-noise) pseudorange and carrier phase dual-frequency observables. The only other data used in the processing were the requisite IGS precise GPS constellation orbit and high-rate GPS constellation clock offset products.

Static Data Testing

The objective of testing with static terrestrial data was to investigate the repeatability of position computations with the technique and to test the performance of the technique against positioning results derived from the highest quality geodetic techniques.

We obtained the data used for this testing from Natural Resources Canada (NRCAN) station Algonquin (IGS station identifier ALGO) in Algonquin Park, Ontario, Canada (latitude 46°N, longitude 78°W). The data spans 24 hours on February 5, 2001. Note that we chose the data set at random. The NRCAN pre-processed receiver output contains measurements with a 30 second sampling interval and a 10° elevation mask angle.

As mentioned previously, the currently un-estimated residual tropospheric delay could cause errors of a few centimeters in the position domain. The receiver

position and clock are estimated at the data sampling interval and this produces a satellite clock modeling error – a few centimeters at the most, arising from interpolating the 300 second interval IGS satellite-clock product. Finally, we have not accounted for Earth orientation, and carrier phase wind-up. These components can also produce centimeter-level errors in position, and we will model them in the near future.

The first aspect of the processing that we analyzed, since this technique relies solely on GPS observations, was the geometric strength of the measurements used. **Figure 3** shows the number of satellites tracked and the position dilution of precision (PDOP). As can be seen, there are always at least 5 satellites being tracked in this data set and on occasion up to 10.

Figure 4 presents the results of the processing. We computed the error

Innovation

values by differencing the estimated position from the benchmark International Earth Rotation Service (IERS), epoch-of-date, International Terrestrial Reference Frame 1997 (ITRF97) coordinates. The error in each component reaches a maximum of ± 50 centimeters. The error fluctuates the most in the vertical component. This is expected, given that we did not estimate the residual tropospheric delay, and given the inherent limitation due to the GPS constellation geometry.

TABLE 1 Summary statistics (centimeters) of component errors in smoothed position estimates for static, terrestrial data set

Component	bias	std.	r.m.s.
North	4.4	13.9	14.5
East	24.3	14.2	14.8
Up	0.6	19.8	19.8
3-D	6.2	28.0	28.7

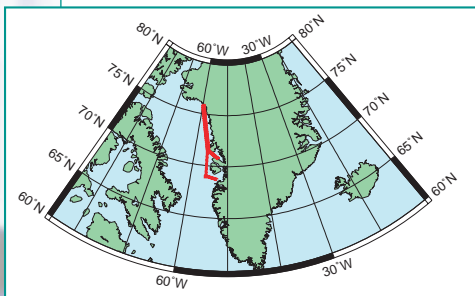


FIGURE 5 Flight path of the aircraft in Greenland in August 2000

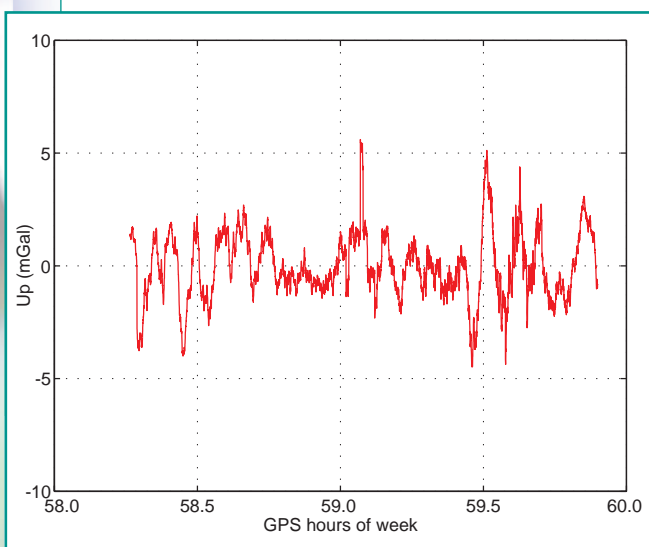


FIGURE 6 Acceleration difference between differential-processing derived and single-receiver derived solutions. Differentiation for acceleration was computed by the third-order central difference of the Taylor series approximation for a 90-second filtering period.

Table 1 gives summary statistics for this data set. The root-mean-square (r.m.s.) error of the smoothed solution is 15 centimeters in each horizontal component, while the vertical component is 20 centimeters. The smoothed total displacement r.m.s. is just less than 30 centimeters. Also of note are the few-centimeter biases that exist in the horizontal components. The standard deviations (std.) give the r.m.s. about the biased mean values. Given that we did not apply the residual tropospheric delay and the sub-daily Earth rotation variations, and that we interpolated the GPS satellite orbits and clocks to 30 seconds, these results are remarkably good, especially compared to typical standalone GPS receiver solutions based on pseudorange-only data. Note that other published precise positioning techniques include dynamic information to constrain the solution space — for example, process noise values indicating a stationary position.

Airborne Data Testing

The next test illustrates the performance of the processing technique for a receiver on a kinematic platform — an airplane in level flight. The technique can be used not only to provide the position of a moving platform, but its velocity and acceleration as well. Accurate determination of aircraft acceleration, for example, is necessary for airborne gravity data processing in support of various applications such as geoid determination, and mineral and fossil fuel exploration.

Total acceleration, measured by accelerometers, is composed of the Earth's gravity field and acceleration due to the motion of the aircraft. Aircraft acceleration can be removed from these measurements based on GPS position estimates. To meet the accuracy requirements, carrier-phase GPS measurements in differential mode are typically used and conventional relative processing techniques applied. The purpose of our test was to investigate a single-receiver approach for airborne positioning, therefore avoiding the

use of additional equipment and data processing. We have compared this technique with relative processing.

We processed GPS data from an airborne gravity campaign, collected in Greenland during August 2000 (see **Figure 5**) with our single-receiver processing software package. We processed the same data estimating the coordinates from vectors to a reference station with a commercial GPS package for comparison. The resulting positions from both packages were twice differenced in time to generate estimates of acceleration.

The equivalence of point and relative positioning acceleration estimates at the milliGal (mGal) level ($1 \text{ mGal} = 10^{-5}$ meters per second squared) shown in **Figure 6** indicates that for the data tested our point positioning technique can be used for airborne gravity determination. The advantages of this single receiver technique can be found in many aspects — such as reduced equipment cost and removal of baseline length constraints.

Spaceborne Data Testing

Spaceborne data is unique for several reasons. The platform carrying the GPS receiver is traveling at very high velocity above the atmosphere which means that the GPS satellites tracked change constantly and there is no tropospheric delay on the received signals. High-fidelity dynamic models are typically required for accurate position and orbit determination (especially for LEOs), and given precise orbits, this data type is an excellent benchmark for mobile receiver positioning.

An example spaceborne data set we have processed consists of twelve hours of CHAMP data from January 5, 2002. This LEO orbits at an approximate altitude of 410 kilometers with a nominal period of 94 minutes, and provides dual-frequency pseudorange and carrier-phase data from a receiver designed at JPL.

The data provided by the CHAMP Data Center is unprocessed and provided at 10 second intervals. Data obtained by the CHAMP receiver in 2001 contain a large number of measurements at extremely low elevation angles. These measurements have very low signal-to-noise values and we found that they produced large position solution errors and large phase residuals. However, at the end of 2001 JPL altered the receiver's tracking algorithm to cease tracking at elevation angles below zero degrees

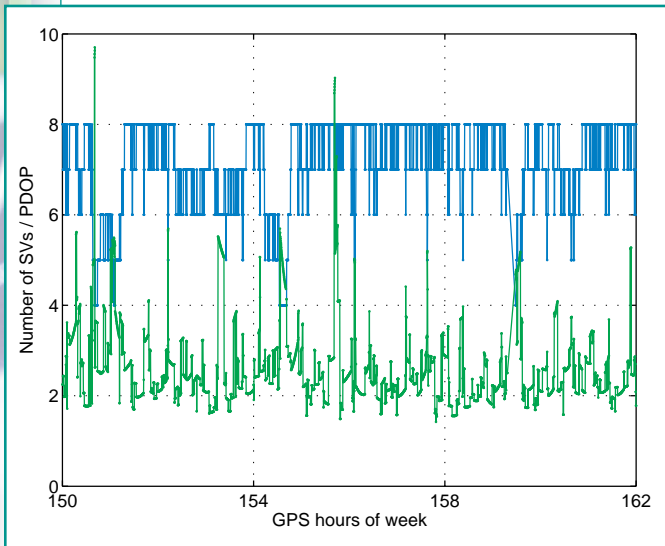


FIGURE 7 Number of SVs and PDOP for the CHAMP spaceborne data set

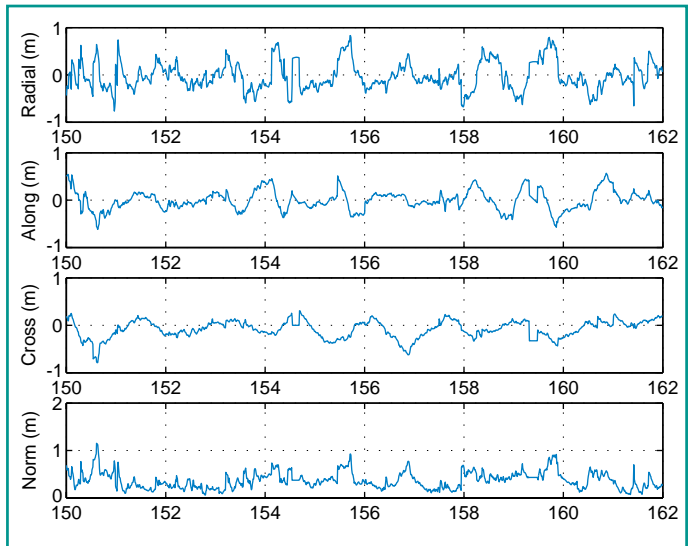


FIGURE 8 Total displacement errors in position estimates for CHAMP spaceborne data set

and the resulting datasets are now much more useful for geometric tracking.

The purpose of processing these test data was to investigate the geometric strength of the spaceborne measurements and to assess the practicality and performance of the technique against high-quality CHAMP orbits. **Figure 7** shows that the geometric strength of the available observations is lower than that for the terrestrial data set we analyzed. The average number of satellites tracked is 7.0. However, there are many more PDOP spikes due to filtered measurement outliers. The mean PDOP is 2.6.

Figure 8 shows the position component differences of our smoothed pseudorange/carrier-phase solution as compared to the GeoForschungsZentrum (GFZ)-determined dynamic orbit. **Table 2** gives the associated summary statistics. Note that the maximum deviation between solution components is below the meter level. The biases are at the few-centimeter level and the overall r.m.s. values are at the 20 centimeter level for the along-track and cross-track components and at the 30 centimeter level for the radial component. These difference statistics are judged to be good consid-

TABLE 2 Summary statistics (in centimeters) of component differences between UNB and GFZ position estimates for CHAMP data set.

Difference	Min.	Max.	Bias	r.m.s.
Radial	-76.4	83.3	-2.2	29.2
Along-track	-61.7	56.6	-0.4	20.5
Cross-track	-79.0	30.7	-8.5	20.1
3-D	5.8	115.0	37.0	41.0

ering that the position accuracy of the dynamic orbit is approximately 15 centimeters in each component. That is, the phase-connected point positioning results have an r.m.s. similar to that of the benchmark solution. A major difference between the solutions is that GFZ's required hours of processing time whereas UNB's required only minutes.

These results compare favorably with those from the terrestrial data set, indicating high-quality observations fitting well with the functional and stochastic models.

Conclusions

Static, terrestrial testing results indicate that near-decimeter position component r.m.s. and few-centimeter position component bias are attainable. These results are seen as promising as there are several improvements that have yet to be made in our software. Airborne results are favourable as well. The spaceborne data testing indicates few-decimeter position component r.m.s. Given all of our test results to date, the goal of decimeter-level position component accuracy

Further Reading

For an earlier discussion of our approach to precise point positioning, see

• "Precise Orbit Determination of Low Earth Orbiters with GPS Point Positioning" by S.B. Bishath and R.B. Langley in *Proceedings of the Institute of Navigation 2001 National Technical Meeting*, Long Beach, California, January 22-24, 2001, pp. 725-733.

For other approaches to single-receiver high-accuracy positioning, see

• "Precise Point Positioning for the Efficient and Robust Analysis of GPS Data From Large Networks" by J.F. Zumberge, M.B. Hefflin, D.C. Jefferson, M.M. Watkins, and F.H. Webb in *Journal of Geophysical Research*, Vol. 102, No. B3, 1997, pp. 5005-5017.

• "Accurate Absolute GPS Positioning Through Satellite Clock Error Estimation" by S.-C. Han, J. H. Kwon, and C. Jekeli in *Journal of Geodesy*, Vol. 75, No. 1, 2001, pp. 33-43.

• "GPS Carrier-Phase Point Positioning with Precise Orbit Products" by P. Héroux, J. Kouba, P. Collins, and F. Lahaye in *Proceedings of the International Symposium on Kinematic Systems in Geodesy, Geomatics and Navigation 2001*, Banff, Alberta, Canada, June 5-8, 2001, pp. 518-528.

For the seminal discussion on combining pseudorange and carrier-phase measurements, see

• "The Synergism of GPS Code and Carrier Measurements" by R. Hatch in *Proceedings of the Third International Geodetic Symposium on Satellite Doppler Positioning*, Las Cruces, New Mexico, February 8-12, 1982, Vol. II, pp.1213-1232.

For the first paper suggesting the use of the kinematic approach to determining the trajectories of spacecraft using GPS, see

• "Strategies for Sub-Decimeter Satellite Tracking with GPS" by T.P. Yunck, S.-C. Wu, and J.-T. Wu in *Proceedings of IEEE Position, Location, and Navigation Symposium 1986*, Las Vegas, Nevada, November 4-7, 1986, pp. 122-128.

is seen as attainable.

Several additional processing and modeling capabilities are required to refine the present strategy and allow for the most accurate position estimates: modeling of sub-daily Earth-rotation variations; phase wind-up; and residual tropospheric delay estimation.

In terms of data processing, more data sets need to be processed to examine the repeatability of these results, and expand the processing capabilities of this technique. Finally, predicted IGS GPS orbits and clocks can be used to attempt real-time precise point positioning.

Acknowledgments

Our research was conducted with support from the Natural Sciences and Engineering Research Council of Canada and the GEOIDE Network of Centres of Excellence. The authors would like to thank the International GPS Service (IGS) for providing the Algonquin Park data set and all of the precise GPS satellite ephemerides and clock offset files; Kort og Matrikelstyrelsen, Denmark for providing the airborne

data set; and the CHAMP Data Center, GeoForschungs- Zentrum, Germany for providing the spaceborne data set. This article is based, in part, on the papers "High-precision Platform Positioning with a Single GPS Receiver" by S.B. Bisnath and R.B. Langley presented at ION GPS 2001, the 14th International Technical Meeting of the Satellite Division of The Institute of Navigation held in Salt Lake City, Utah, September 11-14, 2001 and "Single Receiver GPS Positioning in Support of Airborne Gravity for Exploration and Mapping" by T. Beran, S.B. Bisnath, and R.B. Langley presented at the Third Annual GEOIDE Conference, Fredericton, New Brunswick, June 21-22, 2001. 🌐

Manufacturers

The terrestrial data used to test our software came from the **Allen Osborne Associates, Inc.** (Westlake Village, California) TurboRogue BenchMark receiver at the Algonquin Park IGS site operated by Natural Resources **Canada**. The airborne data was obtained from a **Trimble**

(Sunnyvale, California) 4000ssi GPS receiver. The GPS receiver onboard CHAMP is a **Jet Propulsion Laboratory** (Pasadena, California) BlackJack receiver.



"Innovation" is a regular column featuring discussions about recent advances in GPS technology and its applications as well as the fundamentals of GPS positioning. The column is coordinated by Richard Langley of the Department of Geodesy and Geomatics Engineering at the University of New Brunswick, who appreciates receiving your comments as well as topic suggestions for future columns. To contact him, see the "Columnists" section on page 2 of this issue.